nature neuroscience

Circadian behavior is light-reprogrammed by plastic DNA methylation

Abdelhalim Azzi[1], Robert Dallmann[1], Alison Casserly[1], Hubert Rehrauer[2], Andrea Patrignani[2], Bert Maier[3], Achim Kramer[3] & Steven A Brown[1]

The timing of daily circadian behavior can be highly variable among different individuals, and twin studies have suggested that about half of this variability is environmentally controlled. Similar plasticity can be seen in mice exposed to an altered lighting environment, for example, 22-h instead of 24-h, which stably alters the genetically determined period of circadian behavior for months. The mechanisms mediating these environmental influences are unknown. We found that transient exposure of mice to such lighting stably altered global transcription in the suprachiasmatic nucleus (SCN) of the hypothalamus (the master clock tissue regulating circadian behavior in mammals). In parallel, genome-wide methylation profiling revealed global alterations in promoter DNA methylation in the SCN that correlated with these changes. Behavioral, transcriptional and DNA methylation changes were reversible after prolonged re-entrainment to 24-h d. Notably, infusion of a methyltransferase inhibitor to the SCN suppressed period changes. We conclude that the SCN utilizes DNA methylation as a mechanism to drive circadian clock plasticity.

In mammals, circadian behavior is controlled by the SCN, a group of a few thousand neurons in the ventral hypothalamus. Each cell of these nuclei contains an independent molecular clock based on transcriptional and post-translational feedback loops of dedicated clock proteins[1]. These oscillators have a genetically determined period length of about 24 h and are synchronized to the environment mostly via light. In both rodents and humans, the phase of behavior can vary markedly among different individuals or inbred strains, and these differences carry through to clock function at a cellular level[2,3]. Nevertheless, twin studies suggest that about half of this variability is environmentally controlled[4–6]. Indeed, previous studies have shown that prolonged entrainment to light and dark cycles longer or shorter than 24 h can result in long-lasting changes of the endogenous free-running period (FRP) in rodents[7] and even in humans[8]. At the same time, unexpected lighting has been shown to perturb learning and memory in a fashion dependent on the circadian clock and the retinal ganglion cells that synchronize them to the environment[9]. However, the molecular mechanisms of these changes are unknown.

Until recently, DNA methylation was viewed mostly as a way to permanently silence gene expression during development and differentiation, and it is involved in many biological processes, including imprinting, X-chromosome inactivation and cell differentiation[10]. A number of recent publications in the past few years have shown that changes in DNA methylation in the brain also occur in response to various signals: for example, environmental stress or persistent neural activity change DNA methylation[11,12], and long-term memory seems to require it[13]. This epigenetic modification is catalyzed by a family of enzymes called DNA methyltransferases (DNMTs) and involves the addition of a methyl group to the 5′ position of cytosine residues. The role of this epigenetic modification in regulation of transcription is context dependent. For example, promoter hypo-methylation and gene body hyper-methylation affect transcription positively, whereas promoter methylation generally induces repression of transcription[14].

Recent advances in genomic technologies have allowed researchers to map high-resolution methylation patterns in the genome (the methylome) and have revealed that DNA methylation patterns are more dynamic than previously anticipated. For example, adult mouse dentate granule neurons *in vivo* show a marked and rapid active demethylation or *de novo* methylation 4 h after synchronous neuronal activation[15]. Thus, genomic DNA methylation patterns are highly dynamic, particularly in the brain, and they can be influenced directly by environmental modifications.

To date, there have been no reports on the role of DNA methylation and its effect on gene expression in the process of circadian behavioral plasticity, although a recent report highlighted its possible role in seasonal photoperiodism[16]. We found, to the best of our knowledge, for the first time a direct role for dynamic DNA methylation in the circadian clock, and suggest that this regulation could more generally underlie previously reported effects of altered circadian lighting on mood and memory[9].

RESULTS

Altered day length results in transcriptional changes in the SCN

To explore the mechanism of mammalian circadian plasticity, we exposed 4-week-old mice to different day lengths (T cycles): short days of 22 h (light:dark 11 h:11 h), normal days of 24 h (light:dark 12 h:12 h) or long days of 26 h (light:dark 13 h:13 h). After 6 weeks of

[1]Institute of Pharmacology and Toxicology, University of Zurich, Zurich, Switzerland. [2]Functional Genomics Centre, University of Zurich, Zurich, Switzerland. [3]Laboratory of Chronobiology, Institute of Medical Immunology, Charité Universitätsmedizin, Berlin, Germany. Correspondence should be addressed to S.A.B. (steven.brown@pharma.uzh.ch).

Received 6 August 2013; accepted 17 January 2014; published online 16 February 2014; doi:10.1038/nn.3651

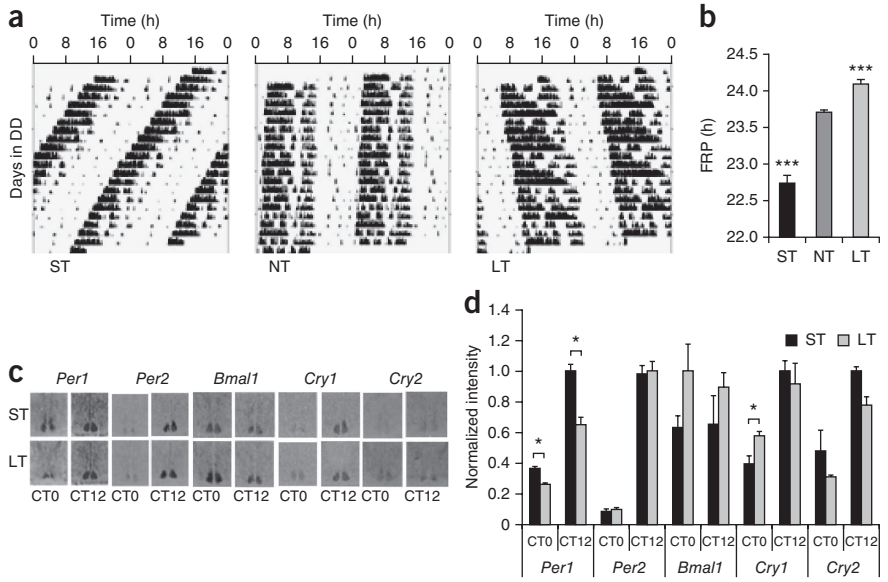

Figure 1 Altered day length in young mice alters the FRP and gene expression in the SCN. (**a**) Representative double-plotted actograms of wheel running activity of mice entrained to 22-h d (ST), 24-h d (NT) and 26-h d (LT) cycles. DD, constant darkness. (**b**) Bar graph showing the FRP recorded from 22-h d, 24-h d and 26-h d mice. Bars represent mean ± s.e.m. ***$P < 0.001$, *post hoc* test of one-way ANOVA, $n = 25$ mice per group. (**c**) Representative autoradiograph of coronal brain sections hybridized with indicated probes, analyzed at CT0 and CT12. (**d**) Bar graph quantifying the level of clock gene mRNA at CT0 (*Per1*, $P = 0.0292$; *Per2*, $P = 0.9940$; *Bmal1*, $P = 0.9351$; *Cry1*, $P = 0.0307$; *Cry2*, $P = 0.9216$) and CT12 (*Per1*, $P = 0.0444$; *Per2*, $P = 0.3565$; *Bmal1*, $P = 2782$; *Cry1*, $P = 0.7758$; *Cry2*, $P = 0.7076$) in mice entrained to 22-h d and 26-h d cycles ($n = 3$–4 mice per CT). *$P < 0.05$, *t* test. Bars represent mean ± s.e.m. See also **Supplementary Figure 5**.

entrainment, we recorded their FRP to monitor their wheel-running activity for 10 d in constant darkness (**Supplementary Fig. 1**). As previously reported[7], subsequent FRP was dependent on the length of day during entrainment (**Fig. 1a**,**b**) and was stable for months in constant conditions (**Supplementary Fig. 2**). Moreover, these effects were age dependent, occurring in younger, but not older, mice (**Supplementary Fig. 3**), and required clock entrainment (**Supplementary Fig. 4**). Changes in FRP were accompanied by changes in both peak and nadir (circadian time (CT) 0 and CT12) values of clock gene expression in the SCN, as determined by *in situ* hybridization (in nocturnal mice, CT0 and CT12 correspond to the time of the activity offset and onset, respectively; **Fig. 1c**,**d** and **Supplementary Fig. 5**).

To gain insight into the effect of aberrant T-cycle lighting on global gene transcription, we focused on the changes occurring in 22-h d mice, where the largest behavioral effects were observed when compared with 24-h d mice. We performed transcriptome sequencing from the SCNs of mice entrained for 4 weeks to 22 h and 24 h d, maintained for a week in darkness, and then killed at CT4 for each mouse. We observed the same changes in clock gene expression as before (**Fig. 1**), notably at *Per* genes and *Cry1* (**Fig. 2a**), which were verifiable by quantitative PCR (qPCR) in different mice (**Fig. 2b**). Notably, changes were also observed globally across the transcriptome at both circadian and non-circadian genes: 171 loci were more than twofold upregulated, and 121 loci were more than twofold downregulated (**Fig. 2c** and **Supplementary Tables 1** and **2**). Enrichment by protein function analysis revealed that these differentially expressed genes were enriched for receptors, ligands and transcription factors (**Fig. 2d**), whereas functional category analysis using DAVID[17] showed that genes involved in aspects of neuronal function and chromatin organization were particularly influenced by T cycle (**Fig. 3**).

In total, our data revealed small steady-state modifications in clock gene levels. In addition, regulated chromatin modifiers included many proteins specifically involved with DNA methylation, such as DNMTs and the Tet (Ten-Eleven Translocation) family, and our transcriptome data showed that most DNA methylation factors themselves, including both maintenance and *de novo* methyltransferases, were expressed in SCN (**Fig. 3b**–**d**).

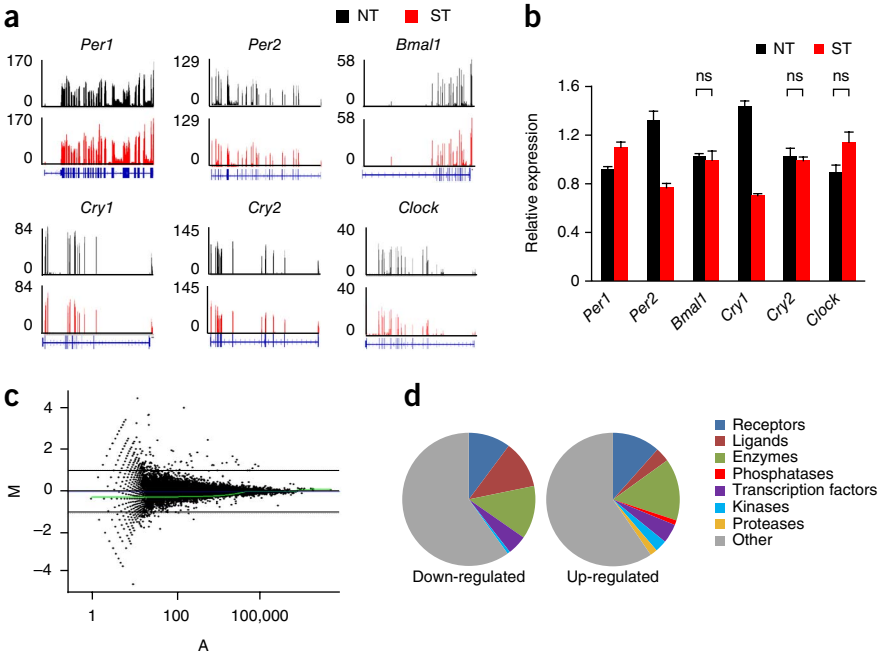

Figure 2 The SCN global transcriptome is altered by day length. (**a**) RNA coverage showing transcript levels of clock genes in SCN transcriptomes of 24-h d and 22-h d mice. (**b**) mRNA levels of clock genes in the SCN, measured by qPCR ($n = 3$ mice per group, bars represent mean ± s.e.m.; unpaired *t* test, ST compared with NT; *Per1*, $P = 0.0189$; *Per2*, $P = 0.0027$; *Bmal1*, $P = 0.7443$; *Cry1*, $P = 0.0001$; *Cry2*, $P = 0.67$). ns indicates not significant ($P > 0.05$). (**c**) Plot of differentially expressed genes identified in SCN transcriptomes of 22-h d mice compared with 24-h d mice. Data represent the $\log_2$ fold-change (M) versus the average $\log_2$ normalized counts (A). Solid lines indicate twofold change threshold. (**d**) Pie chart showing the classification of differentially expressed genes in 22-h d versus 24-h d mice according to their biological function.

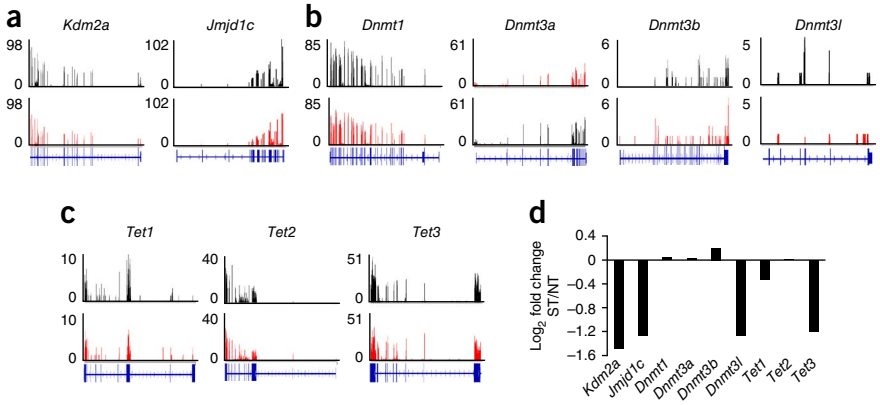

Figure 3 Chromatin-modifying enzymes, histone methyltransferases and their regulators show altered expression during aftereffects of T-cycle exposure. (**a**) RNAseq coverage for chromatin modifiers expressed differentially in 22-h d mice versus 24-h d mice. *Kdm2a*, lysine-specific demethylase 2A; *Jmjd1c*, jumonji domain containing 1C. (**b**,**c**) RNAseq coverage for DNA methyltransferase–related genes: *Dnmt1*, *Dnmt3a*, *Dnmt3b* and *Dnmt3l* and demethylating ten-eleven translocation enzymes *Tet1*, *Tet2*, and *Tet3*. (**d**) Quantification of data presented in **a**–**c**.

Transient epigenetic changes in histone post-translational modification are well-established as important in the circadian clock[18]; however, the idea that more stable modifications in DNA methylation might also be dynamic in adult post-mitotic tissues is new[19]. As discussed above, recent studies have suggested that prolonged changes in steady-state gene expression as a result of behavioral learning or environmental stress are accompanied by changes in DNA methylation in the rodent brain[12,20]. We speculated that this epigenetic modification might provide a mechanism for stable light-dependent circadian clock plasticity.

Altered day length results in global alterations in DNA methylation in the SCN

To test this hypothesis, we isolated genomic DNA from the SCNs of mice entrained to 22- or 24-h d, assessed the methylomes of the two groups using methylated DNA immunoprecipitation (MeDIP), and mapped them using genome-wide promoter tiling arrays. Both our own data and that published by others[21] revealed no significant circadian changes in genomic methylation; however, marked changes were visible in mice exposed to different day lengths. In mice entrained to 22-h d, a total of 1,294 differentially methylated regions (hypo- or hyper-methylated) were identified compared with mice entrained to 24-h d (**Fig. 4a** and **Supplementary Tables 3** and **4**). Process network analysis revealed that both hypo and hypermethylated genes are involved in many neurophysiological processes, including synaptogenesis, axonal guidance and neurohormone signaling (**Supplementary Tables 5** and **6**).

To validate the DNA methylation changes that we observed, we used bisulfite sequencing to confirm the methylation status of two candidate loci (**Fig. 4b**) that were altered in different directions, *Sap30l* (a histone deacetylase complex component, overmethylated in 22-h d mice) and *Avpr2* (a receptor for the hormone arginine vasopressin, undermethylated in 22-h d mice), in SCN DNA samples taken from an independent set of mice. As with the microarray, bisulfite sequencing revealed increased methylation of the *Sap30l* putative promoter and decreased methylation of the *Avpr2* promoter in 22-h d mice compared with 24-h d mice (**Fig. 4c**,**d**). As a final validation, methylation status at these two loci was examined by methylation-dependent restriction enzyme assay. Similar to the previous two assays, increased methylation was observed at the *Sap30l* promoter and decreased methylation was observed at the *Avpr2* promoter under 22-h d conditions. These changes in DNA methylation required prolonged exposure to altered day lengths: 2 weeks of entrainment was not sufficient to alter methylation status using the same assay (**Supplementary Fig. 6**). Moreover, the changes occurred in SCN, but not in cortex, where no differences were observed between 22-h and 24-h d mice at either these loci (**Fig. 4e**) or other genes randomly selected and with different severities of methylation changes (**Supplementary Fig. 7**).

Changes in DNA methylation correlate with transcription

Methylation status of canonical clock genes showed gene- and region-specific alterations in 22-h versus 24-h d mice that correlated with transcriptional changes. Dividing the promoter and downstream region into four regions, increases in *Per2* and *Cry1* promoter methylation (and, in *Cry1*, a sharp decrease in gene body methylation) were accompanied by decreases in SCN transcription, whereas decreases in *Clock* promoter methylation were accompanied by an increase in transcription (**Fig. 4f**). Quantitative PCR analysis also indicated a decrease in mRNA levels of *Sap30l* and increase in mRNA levels of *Avpr2*, nicely mirroring the changes in methylation observed at these loci (**Fig. 4g**). The same correlations were also observed globally. First, overexpressed genes showed significant hypomethylation in promoter regions of 22-h d mice and underexpressed genes showed hypermethyation (**Supplementary Table 7**). Second, Spearman rank of differential methylation versus differential transcription in 22-h and 24-h d mice showed negative correlation (**Fig. 4h**), consistent with the idea that promoter methylation inhibits transcription. Taken together, our data are highly suggestive that dynamic methylation might be causative of the global transcriptome changes that we observed at both circadian and non-circadian genes.

Inhibition of DNA methylation suppresses circadian aftereffects

To validate our hypothesis that dynamic DNA methylation is necessary for circadian aftereffects, we treated mice with the global DNA methyltransferase inhibitor zebularine[22]. Zebularine is a cytidine analog that binds covalently to the active site of DNA methylatransferase enzymes, both enhancing their association with DNA and preventing their disassociation while disrupting their methyltransferase activity[23]. After verifying that we could chronically infuse drugs into the SCN with osmotic pumps (**Supplementary Fig. 8**), we chronically infused mice with zebularine into the third ventricle near the SCN during entrainment to 22-h d. Notably, these mice showed not only a decrease in global and gene-specific DNA methylation in the SCN, but also a marked suppression of FRP changes compared with vehicle-infused mice (percentage of global CpG methylation in mice infused with zebularine deceased compared with vehicle-infused mice: artificial cerebrospinal fluid (aCSF) = 4.67% ± 0.16, zebularine = 3.91% ± 0.15; two tailed, $P = 0.0282$; **Fig. 5a–c**). Moreover, infusion of zebularine also suppressed the previously observed reduction in transcription of *Sap30l* (**Fig. 5d**). Zebularine infusion in constant darkness had no effect on the FRP (**Supplementary Fig. 9**).

From these pharmacological, transcriptomic and methylomic studies, strong evidence can be drawn of a direct correlation between dynamic DNA methylation and circadian aftereffects of altered lighting. To further demonstrate these effects, we studied

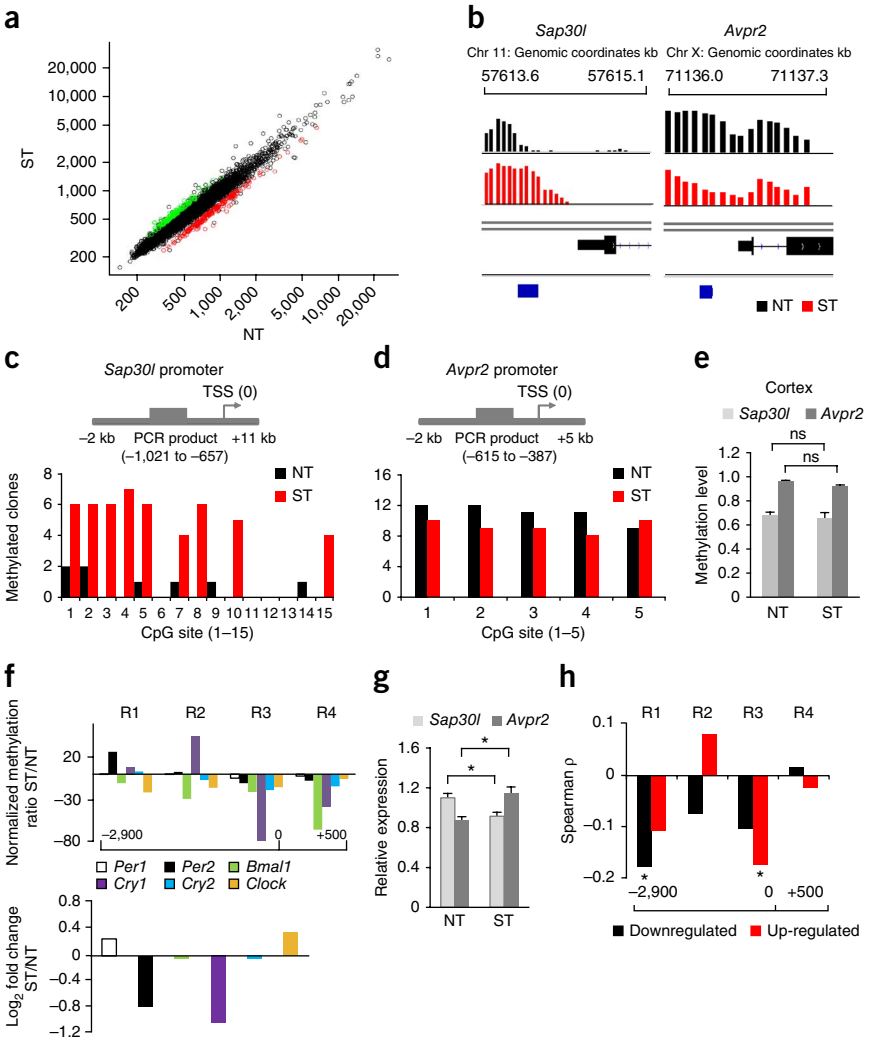

Figure 4 Altered day length induces global changes in DNA methylation in the SCN. (**a**) Scatter plot of the MeDIP:input ratio for whole genome methylation comparison of DNA from 22-h d and 24-h d mice. The red and green dots show hypo- and hyper-methylated genomic regions in 22-h d mice, respectively. (**b**) MeDIP hybridization signals for individual probes on the promoters of *Sap30l* (left) and *Avpr2* (right) loci in SCN of 22-h d (red) and 24-h d (black) mice. Bottom, location of the calculated differentially methylated peak for each locus (blue). (**c**,**d**) Distribution of methylated CpG dinucleotides in the promoter regions of *Sap30l* (left) and *Avpr2* (right), as analyzed by bisulfite sequencing. Genomic regions are indicated on top. *Sap30l* methylation in 24-h d mice = 3.55% ± 1.27, 22-h d mice = 22.22% ± 5.02; two-tailed $P = 0.0012$. *Avpr2* methylation in 24-h d mice = 91.66% ± 3.86; 22-h d mice = 73.33% ± 7.52; two-tailed $P = 0.0412$. (**e**) Methylation levels of *Sap30l* and *Avpr2* in the cortex of 22-h d mice and 24-h d mice, as determined by methylation-dependent restriction enzyme analysis of promoter regions. ns indicates not significant ($P > 0.05$); unpaired *t* test, NT compared with ST; *Sap30l*, $P = 0.6886$; *Avpr2*, $P = 0.0614$. Bars represent mean ± s.e.m. See also **Supplementary Figure 6**. (**f**) Top, percentage change in methylation at different regions of clock gene promoters between 24-h d mice and 22-h d mice, adjusted for overall maximum methylation. Bottom, fold change in transcription of clock genes between 22-h d mice and 24-h d mice, measured at CT4. (**g**) mRNA expression levels of *Sap30l* and *Avpr2* at CT4 in SCNs of 24-h d mice and 22-h d mice, as measured by qPCR ($n = 3$ mice per group, *t* test, ST compared with NT; *Sap30l*, $P = 0.0394$; *Avpr2*, $P = 0.0184$; $^*P < 0.05$). Data are presented as mean ± s.e.m. (**h**) Spearman rank correlation between promoter methylation and expression levels of genes overexpressed (red) and underexpressed (black) in 22-h versus 24-h d lengths. *x* axis shows genomic region relative to transcription start site.

the reversibility of the changes that we observed. We entrained four groups of mice to 22-h and 24-h T cycles for 4 weeks. As before, 4 weeks of entrainment to 22-h induced shortening in the FRP. Re-entrainment to the original T-cycle (24 h) for an additional 4 weeks resulted in a clear reversion in FRP (**Fig. 5e** and **Supplementary Fig. 10**). The plastic changes in circadian behavior (FRP) were accompanied by corresponding alterations and then reversions of methylation levels of *Sap30l* and *Avpr2* (**Fig. 5f**).

DISCUSSION

Overall, our results indicate that the genetically determined period length of the circadian oscillator can be modulated by plastic DNA methylation in the SCN, and provide a simple mechanism to encode a long-term influence of daylight on circadian function. We explicitly explored the effects of altered day lengths on clock plasticity, but the potential mechanism that we explored is wide-reaching. For example, stable methylation of the *frq* gene in *Neurospora* is altered in clock mutants, and reverse DNA methyltransferase mutants show altered circadian period and phase[24]. Similarly, a recent report used a candidate-gene approach to show that DNA methylation of the *dio3* gene is influenced by seasonal effects of light and the hormone melatonin[16]. We found that another altered circadian lighting condition (day length rather than amount of light per day) caused changes not only in circadian behavior, but in global transcription and DNA methylation, and that pharmacological blockage of new DNA methylation suppressed these changes in transcription and behavior. Thus, altered lighting periodicity likely drives changes in DNA methylation to potentially affect many aspects of SCN neurophysiology. In fact, stable methylation changes have been postulated to alter circadian clock properties in response to a wide range of stimuli, including season[16,25], aging[26], shiftwork[27,28], disease[29] and feeding[30]. It is plausible that such changes could underlie negative effects of irregular lighting on long-term memory[9], which are well-documented to require both DNA methylation[22] and circadian clock function[31].

Two important mechanistic questions emerge from our experiments demonstrating the importance of dynamic methylation to circadian plasticity. The first is how altered DNA methylation translates to effects on the circadian clock. On the one hand, the simple methylation of clock genes and the changes in their transcription that we document would be sufficient to explain changes in overall clock function. In *Neurospora,* for example, DNA methylation at the *frq* locus has been shown to have an ancillary role in circadian function[32], modulating both period and phase[24], and the methylation changes that we observed at several clock genes correlated with their

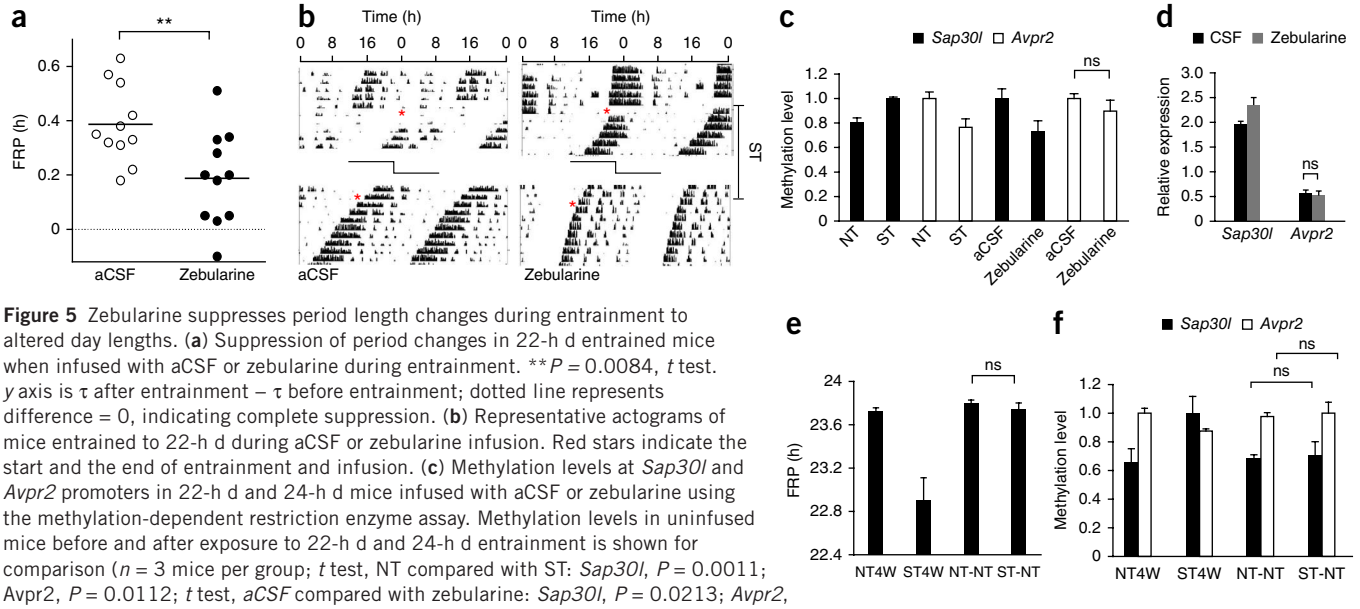

Figure 5 Zebularine suppresses period length changes during entrainment to altered day lengths. (**a**) Suppression of period changes in 22-h d entrained mice when infused with aCSF or zebularine during entrainment. $^{**}P = 0.0084$, *t* test. *y* axis is τ after entrainment – τ before entrainment; dotted line represents difference = 0, indicating complete suppression. (**b**) Representative actograms of mice entrained to 22-h d during aCSF or zebularine infusion. Red stars indicate the start and the end of entrainment and infusion. (**c**) Methylation levels at *Sap30l* and *Avpr2* promoters in 22-h d and 24-h d mice infused with aCSF or zebularine using the methylation-dependent restriction enzyme assay. Methylation levels in uninfused mice before and after exposure to 22-h d and 24-h d entrainment is shown for comparison ($n = 3$ mice per group; *t* test, NT compared with ST: *Sap30l*, $P = 0.0011$; Avpr2, $P = 0.0112$; *t* test, *aCSF* compared with zebularine: *Sap30l*, $P = 0.0213$; *Avpr2*, $P = 0.1511$). Data are presented as mean ± s.e.m. (**d**) mRNA expression levels of *Sap30l* and *Avpr2* at CT4 in SCNs of mice infused with aCSF or zebularine, measured by qPCR ($n = 3$ mice per group; *t* test, *aCSF* compared with zebularine: *Sap30l*, $P = 0.0414$; *Avpr2*, $P = 0.7364$). Data are presented as mean ± s.e.m. (**e**) FRP recorded from mice entrained to only 24-h d for 4 weeks, only 22-h d, 24-h d followed by 24-h d, or 24-h d followed by 22-h d ($n = 5$–6 mice per group, *t* test, NT4W compared with ST4W, $P = 0.0043$; NT-NT compared with ST-NT, $P = 0.3845$). Data are presented as mean ± s.e.m. (**f**) Methylation level of *Sap30l* and *Avpr2* in SCNs of mice harvested after the experiment in **f**, and quantified by methylation-dependent restriction enzyme and qPCR (*t* test, *Sap30l* NT4W compared with ST4W, $P = 0.0262$; NT-NT compared with ST-NT, $P = 0.7529$; *Avpr2* NT4W compared with ST4W, $P = 0.0052$; NT-NT compared with ST-NT, $P = 0.6549$). Data are presented as mean ± s.e.m. ns indicates not significant ($P > 0.05$).

transcriptional changes. To look more broadly in a circadian context, we targeted all of the differentially methylated gene loci by RNAi in cultured U2OS cells, and individually screened them in high-throughput format for effects on circadian dynamics. We found that, when depleted in cells, 5% of all differentially methylated genes affected circadian clock function (Fisher exact test, $P < 0.05$; **Supplementary Fig. 11** and **Supplementary Tables 8–11**). Although the methylated loci were not specifically enriched for genes affecting cell-autonomous circadian function, our results highlight that many other categories of affected genes other than clock genes themselves could also be involved in the observed effects and could affect many behavioral and physiological aspects of the mammalian organism.

A second important question is how changes in day length might translate into the steady-state changes in methylation that we observed. One plausible mechanism would be light-dependent induction or repression of the enzymes catalyzing DNA methylation and demethylation. In support of this idea, many enzymes involved in DNA methylation and demethylation were highly expressed in the SCN, and the expression levels of several were found to be affected by T-cycle (notably *Dnmt3l* and *Tet3*; **Fig. 3b**,**c**,**d**). Exposing mice to a light pulse of 2 h during the subjective night induced substantial changes in RNA levels of these enzymes (**Supplementary Fig. 12**). Regulation of methyltransferase enzymes might also explain why circadian plasticity was observed more strongly in young mice: we observed a strong reduction in DNMT3a protein level in the SCN of 6-month-old mice compared with 6-week-old mice (**Fig. 6**). More broadly, DNA methylation might be a possible mechanism to explain the shift in human chronotype preference observed during aging[33]. However, the older mice also failed to entrain to altered day lengths as effectively, and other hormonal mechanisms have also been proposed to influence circadian aging[34]. Thus, further experiments are needed to ascertain whether defective methylation has a causal role in chronobiological aging.

The idea that stimulus-dependent regulation of methyltransferase expression could globally regulate methylation and circadian plasticity in a variety of contexts is certainly simple and elegant. However, the actual physiologically relevant mechanisms could be substantially more complicated. For example, in the case of memory, the importance of DNA methylation has been clearly demonstrated[20], as has the need for *Tet1*, a member of a family of hydroxymethylases responsible for demethylation[35,36]. In fact, recent research points to temporally specific dynamic DNA methylation and demethylation events in response to upstream signaling cascades[37]. The degree

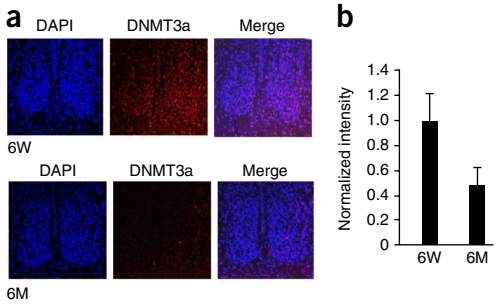

Figure 6 DNMT3a protein expression decreases with aging. Six-week-old (6W) and 6-month-old (6M) mice were raised under normal day lengths (24-h d) and then transferred to constant darkness for two consecutive days. Brains were then collected at CT6. Coronal brain sections were prepared via microtome and stained for DNMT3a using rabbit polyclonal antibody to DNMT3a (ab2850, Abcam) ($n = 4$ mice per group). (**a**) Example of two SCNs sections stained with DAPI for nuclei and DNMT3a from six-week-old and six-month-old mice. (**b**) Normalized intensity levels of DNMT3a expression in the same group of mice (*t* test, $P = 0.0225$). Data are presented as mean ± s.e.m.

to which methylation-dependent circadian plasticity parallels this mechanism remains to be established. For example, remote fear memory can be erased immediately after treatment with DNMT inhibitors[38], whereas plastic circadian changes were not reversed in a similar experiment. Two groups of mice were entrained to 22-h d for 4 weeks, received a single injection of zebularine or vehicle (aCSF), and then transferred to constant darkness for FRP measurement. Single injection of zebularine after entrainment to 22-h d did not revert shortening in the FRP of these mice, hinting that a more complicated reversal program was needed (**Supplementary Fig. 13**). It is also not clear whether the methylation changes that we observed are needed to establish the circadian clock changes or also to maintain them. Finally, it should be noted that, although zebularine is a specific inhibitor of DNA methyltransferases (as opposed to histone methyltransferases), it also has acts on cytosine deaminases[39], indicating that additional indirect effects could be involved.

In general, however, the mechanisms that we describe essentially unclench global changes in transcriptome and methylome as a result of altered lighting, and these changes could be involved in a large variety of neurophysiological process, including mood, learning and memory. Indeed, in addition to the circadian clock, we found that a substantial number of differentially methylated genes are important in synaptogensis, axon guidance and neurohormone signaling. Thus, our results suggest that a stable early-life circadian lighting environment could be important for health. Conversely, targeting these epigenetic changes could suppress nefarious long-term consequences of altered lighting or allow human beings to better adapt to conditions such as space travel or shiftwork.

METHODS

Methods and any associated references are available in the online version of the paper.

Accession codes. The raw sequence data obtained by RNA-seq are available at the NCBI Gene Expression Omnibus under series accession number GSE54124. The raw array data obtained by MeDIP-array are available at the NCBI Gene Expression Omnibus UNDER series accession number GSE54021.

Note: Any Supplementary Information and Source Data files are available in the online version of the paper.

ACKNOWLEDGMENTS

This work was supported by the Velux Foundation, the Swiss National Science Foundation and the Zürich Clinical Research Program 'Sleep and Health'. A.A. and S.A.B. are members of the Zürich Neurozentrum graduate program, and S.A.B. is also a member of the Molecular Life Sciences program. R.D. is a Feodor Lynen Fellow of the Humboldt Foundation.

AUTHOR CONTRIBUTIONS

A.A. and A.C. performed all experiments, with assistance from R.D., H.R. and A.P. Knockdown experiments in U2OS cells were performed and analyzed by B.M. with assistance from A.K. Data analysis was conducted by A.A., R.D., H.R., B.M. and A.P. The paper was written by A.A., R.D., B.M., A.K. and S.A.B.

COMPETING FINANCIAL INTERESTS

The authors declare no competing financial interests.

1. Dibner, C., Schibler, U. & Albrecht, U. The mammalian circadian timing system: organization and coordination of central and peripheral clocks. *Annu. Rev. Physiol.* **72**, 517–549 (2010).
2. Brown, S.A. *et al.* The period length of fibroblast circadian gene expression varies widely among human individuals. *PLoS Biol.* **3**, e338 (2005).
3. Brown, S.A. *et al.* Molecular insights into human daily behavior. *Proc. Natl. Acad. Sci. USA* **105**, 1602–1607 (2008).
4. Barclay, N.L., Eley, T.C., Buysse, D.J., Archer, S.N. & Gregory, A.M. Diurnal preference and sleep quality: same genes? A study of young adult twins. *Chronobiol. Int.* **27**, 278–296 (2010).
5. Hur, Y.M. Stability of genetic influence on morningness-eveningness: a cross-sectional examination of South Korean twins from preadolescence to young adulthood. *J. Sleep Res.* **16**, 17–23 (2007).
6. Koskenvuo, M., Hublin, C., Partinen, M., Heikkila, K. & Kaprio, J. Heritability of diurnal type: a nationwide study of 8753 adult twin pairs. *J. Sleep Res.* **16**, 156–162 (2007).
7. Pittendrigh, C.S. & Daan, S. A functional analysis of circadian pacemakers in nocturnal rodents. *J. Comp. Physiol.* **106**, 223–252 (1976).
8. Chang, A.M., Scheer, F.A. & Czeisler, C.A. The human circadian system adapts to prior photic history. *J. Physiol. (Lond.)* **589**, 1095–1102 (2011).
9. LeGates, T.A. *et al.* Aberrant light directly impairs mood and learning through melanopsin-expressing neurons. *Nature* **491**, 594–598 (2012).
10. Bird, A. DNA methylation patterns and epigenetic memory. *Genes Dev.* **16**, 6–21 (2002).
11. Guo, J.U. *et al.* Neuronal activity modifies the DNA methylation landscape in the adult brain. *Nat. Neurosci.* **14**, 1345–1351 (2011).
12. Murgatroyd, C. *et al.* Dynamic DNA methylation programs persistent adverse effects of early-life stress. *Nat. Neurosci.* **12**, 1559–1566 (2009).
13. Day, J.J. & Sweatt, J.D. DNA methylation and memory formation. *Nat. Neurosci.* **13**, 1319–1323 (2010).
14. Ball, M.P. *et al.* Targeted and genome-scale strategies reveal gene-body methylation signatures in human cells. *Nat. Biotechnol.* **27**, 361–368 (2009).
15. Molyneux, P.C., Dahlgren, M.K. & Harrington, M.E. Circadian entrainment aftereffects in suprachiasmatic nuclei and peripheral tissues *in vitro*. *Brain Res.* **1228**, 127–134 (2008).
16. Stevenson, T.J. & Prendergast, B.J. Reversible DNA methylation regulates seasonal photoperiodic time measurement. *Proc. Natl. Acad. Sci. USA* **110**, 16651–16656 (2013).
17. Huang, D.W., Sherman, B.T. & Lempicki, R.A. Systematic and integrative analysis of large gene lists using DAVID Bioinformatics Resources. *Nat. Protoc.* **4**, 44–57 (2009).
18. Masri, S. & Sassone-Corsi, P. The circadian clock: a framework linking metabolism, epigenetics and neuronal function. *Nat. Rev. Neurosci.* **14**, 69–75 (2013).
19. Franchini, D.M., Schmitz, K.M. & Petersen-Mahrt, S.K. 5-Methylcytosine DNA demethylation: more than losing a methyl group. *Annu. Rev. Genet.* **46**, 419–441 (2012).
20. Miller, C.A. *et al.* Cortical DNA methylation maintains remote memory. *Nat. Neurosci.* **13**, 664–666 (2010).
21. Vollmers, C. *et al.* Circadian oscillations of protein-coding and regulatory RNAs in a highly dynamic mammalian liver epigenome. *Cell Metab.* **16**, 833–845 (2012).
22. Miller, C.A. & Sweatt, J.D. Covalent modification of DNA regulates memory formation. *Neuron* **53**, 857–869 (2007).
23. Champion, C. *et al.* Mechanistic insights on the inhibition of c5 DNA methyltransferases by zebularine. *PLoS ONE* **5**, e12388 (2010).
24. Belden, W.J., Lewis, Z.A., Selker, E.U., Loros, J.J. & Dunlap, J.C. CHD1 remodels chromatin and influences transient DNA methylation at the clock gene frequency. *PLoS Genet.* **7**, e1002166 (2011).
25. Ciarleglio, C.M., Axley, J.C., Strauss, B.R., Gamble, K.L. & McMahon, D.G. Perinatal photoperiod imprints the circadian clock. *Nat. Neurosci.* **14**, 25–27 (2011).
26. Zhang, L. *et al.* Tissue-specific modification of clock methylation in aging mice. *Eur. Rev. Med. Pharmacol. Sci.* **17**, 1874–1880 (2013).
27. Shi, F. *et al.* Aberrant DNA methylation of miR-219 promoter in long-term night shiftworkers. *Environ. Mol. Mutagen.* **54**, 406–413 (2013).
28. Zhu, Y. *et al.* Epigenetic impact of long-term shiftwork: pilot evidence from circadian genes and whole-genome methylation analysis. *Chronobiol. Int.* **28**, 852–861 (2011).
29. Milagro, F.I. *et al.* CLOCK, PER2 and BMAL1 DNA methylation: association with obesity and metabolic syndrome characteristics and monounsaturated fat intake. *Chronobiol. Int.* **29**, 1180–1194 (2012).
30. Maekawa, F. *et al.* Diurnal expression of Dnmt3b mRNA in mouse liver is regulated by feeding and hepatic clockwork. *Epigenetics* **7**, 1046–1056 (2012).
31. Levenson, J.M. *et al.* Evidence that DNA (cytosine-5) methyltransferase regulates synaptic plasticity in the hippocampus. *J. Biol. Chem.* **281**, 15763–15773 (2006).
32. Ciarleglio, C.M., Axley, J.C., Strauss, B.R., Gamble, K.L. & McMahon, D.G. Perinatal photoperiod imprints the circadian clock. *Nat. Neurosci.* **14**, 25–27 (2011).
33. Roenneberg, T. *et al.* A marker for the end of adolescence. *Curr. Biol.* **14**, R1038–R1039 (2004).
34. Pagani, L. *et al.* Serum factors in older individuals change cellular clock properties. *Proc. Natl. Acad. Sci. USA* **108**, 7218–7223 (2011).
35. Kaas, G.A. *et al.* TET1 controls CNS 5-methylcytosine hydroxylation, active DNA demethylation, gene transcription, and memory formation. *Neuron* **79**, 1086–1093 (2013).
36. Rudenko, A. *et al.* Tet1 is critical for neuronal activity-regulated gene expression and memory extinction. *Neuron* **79**, 1109–1122 (2013).
37. Zovkic, I.B., Guzman-Karlsson, M.C. & Sweatt, J.D. Epigenetic regulation of memory formation and maintenance. *Learn. Mem.* **20**, 61–74 (2013).
38. Franchini, D.M., Schmitz, K.M. & Petersen-Mahrt, S.K. 5-Methylcytosine DNA demethylation: more than losing a methyl group. *Annu. Rev. Genet.* **46**, 419–441 (2012).
39. Lemaire, M., Momparler, L.F., Raynal, N.J., Bernstein, M.L. & Momparler, R.L. Inhibition of cytidine deaminase by zebularine enhances the antineoplastic action of 5-aza-2′-deoxycytidine. *Cancer Chemother. Pharmacol.* **63**, 411–416 (2009).

ONLINE METHODS

Mice. All mouse experiments were conducted in accordance with applicable veterinary law, using wild-type mice (C57BL/6J) and were approved by the Zurich cantonal veterinary office. In experiments for which activity was measured before and after entrainment, 4-week-old mice were housed in the presence of running wheels for 3 d, and then running wheel activity was measured in constant darkness for 1 week. Subsequently, mice were exposed to either 22-h d (light:dark, 11 h:11 h), 24-h d (light:dark, 12 h:12 h) or 26-h d (light:dark, 13 h:13 h) for 4 weeks, and then running wheel activity was measured for an additional 10 d in constant darkness. Deviations from this basic protocol are described for each experiment where necessary below. Circadian period was determined from running wheel usage patterns using the ClockLab software package (Actimetrics).

***In situ* hybridization analysis.** We exposed two groups of 3-week-old mice to 22-h d and 26-h d. After 6 weeks, we recorded wheel-running behavior in constant darkness. After 3 d in constant darkness, we used Clocklab software (Actimetrics) to predict time of activity onset for each mouse (defined as circadian time CT12), and one half-cycle after activity onset (defined as CT0). Brains were isolated at the indicated circadian time point and sliced with a cryostat (thickness, 12 µM). *In situ* hybridization analysis was performed as described previously[40], using full-length cRNA probes.

RNAseq analysis. First, 16 5–6-week-old mice were exposed to constant darkness for 7 d to measure their FRP. Then, mice were separated into two groups of eight and entrained to 22-h d and 24-h d. After 4 weeks, we recorded wheel-running behavior in constant darkness. After 5 d in constant darkness, we used Clocklab software to predict time of activity onset for each mouse. Brains were isolated at CT4 and sliced with a microtome using a fresh HBSS medium (thickness = 250 µm) and the SCN was cut out with the aid of a binocular microscope and stored immediately at −80 °C. Total RNA was extracted using the SurePrep Nuclear or Cytoplasmic RNA Purification Kit (Fisher Scientific) according to the manufacturer's protocol. A total of 500 ng of RNA was used for subsequent steps. These steps included DNAase treatment, polyA selection, depletion of ribosomal RNA, overall quality check and library preparation, and were performed by Fasteris (CH). Libraries were prepared according to standard Illumina protocols.

Sequence quality, read mapping and data analysis. All steps were done using the GeneProf platform[41]. Briefly, the sequencing reads of each library were first quality checked for read length and nucleotide composition, and then submitted for mapping to the mouse genome reference sequence (Ensemble 58 mouse Genes, NCBIM37 assembly) using the alignment tool TopHat[42]. Quantitative and differential gene expression was carried out using the Deseq package[43] using default parameters. To identify the top differentially expressed genes, we used a twofold cutoff to the average change in gene expression ($\log_2 \geq 1$) and eight reads as cutoff for minimum number of reads per gene. Read coverage and visualization were done using Integrative Genomics Viewer (IGV) software[17].

Isolation of DNA from SCN and MeDIP-array. For methyl-DNA immunoprecipitation (MeDIP), we adapted a previously described protocol[44]. First, we exposed two groups of 3-week-old mice to 22-h d and 24-h d (n = 25 mice per group). After 6 weeks, we recorded wheel-running behavior in constant darkness for 1 week and then isolated brains and sliced them with a vibratome. Brain slices (70 µm) were stained with cresyl-violet to identify SCN tissue. Genomic DNA was extracted from SCN slices by overnight Proteinase K digestion, followed by phenol-chloroform and ethanol precipitation. After RNase treatment, intact genomic DNA was sonicated to generate small fragments (average = 500 bp), using a Covaris sonicator (BioRuptor). Sonicated DNA was denatured for 10 min at 95 °C. For immunoprecipitation, we used 1.5 µg of denatured DNA with 2 µg of monoclonal antibody to 5-methylcytidine (BI-MECY-0100, Eurogentec) for 3 h at 4 °C. The mixture (DNA plus antibody) was incubated with 30 µl of protein A-sepharose during 2 h at 4 °C. After washing, beads were resuspended in 250 µl of elution buffer and incubated 3 h at 55 °C on a rotating wheel. The immunoprecipitated DNA was then submitted to phenol/chloroform extraction and ethanol precipitation. To evaluate the specificity and the efficiency of the immunoprecipitation, we used primers for known methylated and unmethylated regions as positive and negative controls (**Supplementary Table 6**). Real-time PCR analyses were performed using the AB Prism 7900 real time PCR machine (Applied Biosystems) and Eva Green Master Mix (Biotium). Primers are listed below. The reactions were carried out in triplicate. Relative enrichment for positive and negative control is expressed as the ratio of signal in the immunoprecipitated DNA to the input DNA, and was 0.8 for positive control and 0.004 for negative control genomic regions. Subsequent genome-wide analysis is described further below.

Promoter and CpG island array hybridization and analysis. For genome-wide methylation analysis, we used 10 ng of input DNA and immunoprecipitated DNA for library preparation and DNA amplification using GenomPlex complete whole genome amplification WGA2 (Sigma). For labeling, we used 1 µg of DNA (input and immunoprecipitate) with Cy5 and Cy3 using the dual-color labeling kit (Roche). Labeled DNA was used for hybridization to the Mouse DNA Methylation 3x720K CpG Island Plus RefSeq Promoter Arrays (Nimblegen). Hybridization and washing were carried out according the manufacturer's instructions. To find differentially methylated regions between 24-h d and 22-h d mice, we used the SLAM software (GausSian nonlinear Analysis of MeDIP-chip data) as performed previously[45]. For data normalization and background subtraction, we used the MA2C method[46]. Result were visualized using IGV[17]. Process network analysis of the differentially methylated regions between 24-h d and 22-h d was done using GeneGo MetaCore Pathway Analysis Software.

Region-specific methylation changes between 22-h d and 24-h d (**Fig. 3**) were quantified as the ratio of average methylation across all probes in the region under the two conditions, multiplied by 100 and then by the maximum methylation in the region, to furnish a weighted score that penalizes large fold changes at essentially unmethylated regions.

Intra-cerebroventricular infusion of zebularine. Zebularine (Berry and Associates, cat no. PY7715) was dissolved in DMSO to a concentration stock of 500 mM and diluted in aCSF for infusion into the third ventricle. To ensure that we could reliably chronically infuse zebularine into the third ventricle in a way that pharmacologically influences the SCN, we performed a control experiment in which mice were chronically infused with TGFα for 7 d using ALZET osmotic mini pump model 1007D as described[47], and suppression of locomotor changes were observed as published previously (**Supplementary Fig. 7**). Next, to quantify the effects of the DNA methyltransferase inhibitor zebularine on circadian aftereffects, 6-week-old mice were exposed to constant darkness for 10 d to record their FRP. Osmotic mini pump model 1004 (ALZET) was used to infuse zebularine (1 µg µl^{-1}) or aCSF at a rate of 0.11 µl h^{-1} for 28 d. After surgery mice were entrained to 11 h:11 h (short day) conditions for 28 d under chronic infusion of zebularine or CSF, and then released in constant darkness for 10 d to record their FRP. For stereotaxic surgery, mice were anesthetized and fixed in a Kopf stereotact. A stainless steel needle connected to a catheter was aimed at the third ventricle (relative to bregma: AP: −0.22 mm, ML: ±0.25 mm, DV: 4 mm). Needle placement was confirmed *post mortem* optically by serial coronal sectioning (**Supplementary Fig. 7**).

Bisulfite sequencing. To confirm the difference in methylation between 22-h d and 24-h d mice, we used another set of mice for bisulfite sequencing than that used for MeDIP experiments. 3-week-old mice were entrained to 22-h d and 24-h d for 6 weeks (6 mice per group). Brains were isolated and sectioned coronally. After cresyl violet staining, SCNs were isolated as described above. DNA from SCN was subjected to bisulfite conversion with the EZ DNA Methylation Kit (Zymo Research) and purified following the manufacturer's instructions. Purified DNA was PCR amplified using BSP primers. PCR products were purified using gel extraction kit (Qiagen) and cloned into PGEM vector using the TOPO TA Cloning Kit (Promega). Positive clones were sequenced by Microsynth AG.

RT-qPCR analysis. Transcription analysis of the indicated genes was performed using another independent set of mice, using a protocol described previously[48]. Primers for candidate genes are described below. Primers for circadian clock genes are described elsewhere[49].

Methylation-dependent restriction enzyme and real-time PCR. Genomic DNA was isolated from the SCN of 24-h d and 22-h d and mice infused with aCSF and zebularine, and 100 ng of each was subjected to digestion with the enzyme McrBC

or no enzyme as a control. To control for digestion efficiency, we used plasmids methylated and unmethylated *in vitro* in the same assay. For more details, see ref. 50. Primers are described below.

Global DNA methylation analysis. The global CpG methylation measurement in mice infused with aCSF or zebularine was carried out using the colorimetric method using MethyFlash Methylated DNA quantification Kit (Epigentek) according to the manufacturer's instructions.

Immunohistochemistry staining. 6-week-old and 6-month-old mice were under 24-h d and then transferred to constant darkness for two consecutive days. Brains were then collected at CT6. Coronal brains section of 20 μM thickness were prepared with microtome. Slices were fixed with 4% paraformaldehyde (wt/vol) for 15 min and then washed three times with PBS. They were then permeabilized with permeabilization buffer (PBS + 0.3% Triton X-100, vol/vol) for 30 min at 20 °C, and then washed three time with wash buffer (PBS + 0.05% Triton X-100). After blocking in PBS + 0.05% Triton X-100 supplemented with 3% powdered non-fat milk (wt/vol), tissue sections were incubated overnight with primary antibody to DNMT3a (1: 500, (ab2850, Abcam) in blocking solution. Secondary antibody (Alexa 680, Cy3-conjugated) was used at dilution of 1: 200 in blocking solution for fluorescence detection. During the last wash sections were stained also with DAPI to visualize cell nuclei.

RNAi analysis. Differentially expressed and differentially methylated genes were silenced in U2OS cells via RNAi using 1–8 separate hairpin sequences (Open Biosystems) per gene. Circadian clock effects were measured via a circadian Bmal-luciferase reporter as described[51].

MeDIP primers. For positive control region, IAP transposon primers were forward 5′-CTCCATGTGCTCTGCCTTCC-3′ and reverse 5′-CCCCGTCC CTTTTTTAGGAGA-3′. For negative control region, β-actin, primers were forward 5′-AGCCAACTTTACGCCTAGCGT-3′ and reverse 5′-TCTCAAGAT GGACCTAATACGGC-3′.

Methylation-dependent restriction enzyme primers. For *Sap30l*, primers were forward 5′-TGCCCGCTGTACTCAAAGATT-3′ and reverse 5′-GC CTGGGCTGGAGGATCTAC-3′. For *Avpr2*, primers were forward 5′-G GTGCGTGAGGGAAAGGA-3′ and reverse 5′-TTTTGTAGCCCCTTACCT GCTT-3′.

Bisulfite sequencing primers. For *Sap30l*, primers were forward 5′-TTTTGAAG ATTAATTTAGGTTAGGGTT-3′ and reverse 5′-AAAACAAACTTACAACAAA AATCAC-3′. For *Avpr2*, primers were forward 5′-TTTATTTTTTGGTAGATGG AGGAAG-3′ and reverse 5′-TCAAAACTCTTTTATAACCCCTTACC-3′.

RT-qPCR primers. For *Sap30l*, primers were forward 5′-GAACACGCTC CGACGTTACA-3′ and reverse 5′-GGCAAGCGTCTCTTTCTCATTC-3′. For *Avpr2*, primers were forward 5′-GCTGGCTAGCCTTAACAGCTGTA-3′ and reverse 5′-CGCAACTCCGAGGAGACACT-3′.

Statistics. Data were analyzed with Microsoft excel and Prism (GraphPad Software). Sample sizes were determined on the basis of similar experiments performed by others, and modified as necessary in subsequent biological replicates based on observed outcome. Experiments were either performed blinded, or else data was cross-checked by blinded co-investigators. For behavior, all data from different experimental conditions were collected simultaneously in randomly assigned measurement stations. For biochemistry and genomics, all experimental conditions were processed in parallel simultaneously. Where appropriate, data was examined for normality via normal probability plotting. For comparison of more than two groups, one-way ANOVA was used. Where specified, non-parametric tests were also used (Wilcoxon signed-rank comparison test in case of **Supplementary Table 7**).

40. Brown, S.A., Zumbrunn, G., Fleury-Olela, F., Preitner, N. & Schibler, U. Rhythms of mammalian body temperature can sustain peripheral circadian clocks. *Curr. Biol.* **12**, 1574–1583 (2002).
41. Halbritter, F., Vaidya, H.J. & Tomlinson, S.R. GeneProf: analysis of high-throughput sequencing experiments. *Nat. Methods* **9**, 7–8 (2012).
42. Trapnell, C., Pachter, L. & Salzberg, S.L. TopHat: discovering splice junctions with RNA-Seq. *Bioinformatics* **25**, 1105–1111 (2009).
43. Anders, S. & Huber, W. Differential expression analysis for sequence count data. *Genome Biol.* **11**, R106 (2010).
44. Weber, M. *et al.* Chromosome-wide and promoter-specific analyses identify sites of differential DNA methylation in normal and transformed human cells. *Nat. Genet.* **37**, 853–862 (2005).
45. Rai, K. *et al.* DNA demethylase activity maintains intestinal cells in an undifferentiated state following loss of APC. *Cell* **142**, 930–942 (2010).
46. Song, J.S. *et al.* Model-based analysis of two-color arrays (MA2C). *Genome Biol.* **8**, R178 (2007).
47. Kramer, A. *et al.* Regulation of daily locomotor activity and sleep by hypothalamic EGF receptor signaling. *Science* **294**, 2511–2515 (2001).
48. DeBruyne, J.P., Weaver, D.R. & Reppert, S.M. CLOCK and NPAS2 have overlapping roles in the suprachiasmatic circadian clock. *Nat. Neurosci.* **10**, 543–545 (2007).
49. Kowalska, E. *et al.* Distinct roles of DBHS family members in the circadian transcriptional feedback loop. *Mol. Cell. Biol.* **32**, 4585–4594 (2012).
50. Oakes, C.C., La Salle, S., Robaire, B. & Trasler, J.M. Evaluation of a quantitative DNA methylation analysis technique using methylation-sensitive/dependent restriction enzymes and real-time PCR. *Epigenetics* **1**, 146–152 (2006).
51. Maier, B. *et al.* A large-scale functional RNAi screen reveals a role for CK2 in the mammalian circadian clock. *Genes Dev.* **23**, 708–718 (2009).

doi:10.1038/nn.3651